ISSN 0967-0912, Steel in Translation, 2017, Vol. 47, No. 6, pp. 363–368. © Allerton Press, Inc., 2017.
Original Russian Text © V.N. Shinkin, 2017, published in Izvestiya Vysshikh Uchebnykh Zavedenii, Chernaya Metallurgiya, 2017, No. 6, pp. 436–442.

Failure of Large-Diameter Steel Pipe with Rolling Scabs

V. N. Shinkin

Moscow Institute of Steel and Alloys, Moscow
e-mail: shinkin-korolev@yandex.ru

Received May 25, 2017

Abstract—Russian pipelines employ large-diameter pipe of straight-seam, two-seam, and spiral-seam type (diameter up to 1420 mm, API strength class up to K65). The newest developments in the production of large-diameter (1020, 1220, and 1420 mm) straight-seam welded pipe (strength classes K38–K65 and X42– X80, wall thickness up to 52 mm, length up to 18 mm, and working pressure up to 22.15 MPa) is stepwise press shaping (the JCOE process), proposed by SMS Meer (Germany). The SMS Meer technology is widely used at Russian pipe plants (AO Vyksunskii Metallurgicheskii Zavod, AO Izhorskii Trubnyi Zavod, PAO Chelyabinskii Truboprokatnyi Zavod) and also plants in Russia, China, and India. However, the accident statistics for Russian pipelines show that stress corrosion of the pipe wall mainly occurs in pipelines of large diameter (700–1420 mm). More than 80% of pipeline failures associated with stress corrosion occur in pipelines of diameter 1020–1420 mm. Corrosion cracking of pipe walls may be attributed to three main factors: (1) poor steel quality and pipe defects in manufacturing (such as high residual stress, microcracks and micropeeling of the metal after shaping of the pipe blank, corrugation, scratches, scabs from the rolling process, and imperfections of the weld seams); (2) the presence of a corrosive medium and its access to the metal surface; (3) multicyclic fatigue and failure of the metal on account of pulsation of the working pressure within the pipe and hydraulic shocks. In Russian oil pipelines, failures due to production defects and assembly and installation problems are twice as frequent as in the United States and Europe. Therefore, careful study of pipeline failure due to production flaws is of great importance. In the present work, a mathematical approach is proposed to determining the critical pressure in the pipe at which elastoplastic failure of the pipe will occur at rolling scabs accompanied by a scratch on the pipe's outer surface. The results may be used in failure diagnostics of large-and medium-diameter steel pipe for major delivery pipelines and transfer pipelines.

Keywords: large-diameter welded steel pipe, medium-diameter welded pipe, critical pipe-failure pressure, rolling scab, surface scratches, major pipelines, transfer pipelines, elastoplastic media, linear strengthening

DOI: 10.3103/S0967091217060109

The manufacture of large-diameter steel pipe for major pipelines includes numerous mechanical and thermomechanical processes, such as hot rolling of high-strength steel slabs and broad strip; controlled capillary–drop and laminar cooling to increase the strength and reduce the grain size of the steel; straightening of steel strip and sheet on multiroller machines to reduce the waviness and buckling of the blank; trimming of the edges of strip and sheet by guillotines and disk cutters; shaping of the sheet on presses; and correction of the diameter of the pipe blank on expanders [1–36].

PIPELINE ACCIDENTS

Between 1999 and 2009, the mean annual incidence of accidents per 1000 km of major Russian pipelines was 0.06. In Western Europe, the corresponding figure between 1991 and 2006 was 0.32; for North America, the figure was 0.48.

In Europe, the three factors responsible for most accidents and leaks are external disturbances (36%), stress corrosion (29%), and mechanical damage (24%).

The corresponding factors for Russian pipelines (according to 2001–2006 data) are external disturbances (34.3%), installation and construction problems (23.2%), stress corrosion (22.5%), smelting and pipe-production defects (14.1%), and human error (3%) [18–20].

Annually, out of the 305 million t of petroleum extracted in Russia, there will be losses of 10–15 million t (about 4–5%) from pipelines on account of stress corrosion (corrosional cracking under stress) and cyclic pressure differences within the pipe. The annual losses from direct petroleum losses alone reach $270 million. The density of stress-corrosion defects in major pipelines is 14.6 per km. Overall, the rate of stress corrosion is 0.2–0.5 mm/yr, but it increases in some regions to 0.8–1.16 mm/yr.

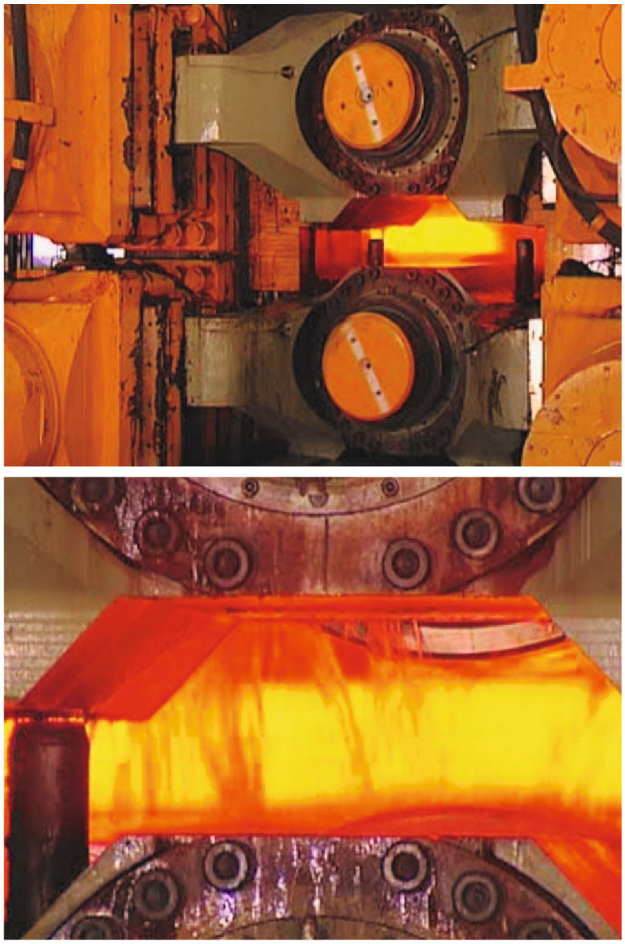

Fig. 1. Hot steel strip between rollers in a mill.

Between 1991 and 2001, stress corrosion was responsible for 22.5% of all accidents in Russian gas pipelines; for 2000, the figure was 37.4%.

In addition, 350000 km of transfer pipelines are in operation in Russia. Each year, more than 50000 hazardous incidents accompanied by oil spills are noted at those pipelines, mainly on account of stress corrosion of the pipe. The wear of the transfer pipelines is as much as 80%. Their failure frequency is two orders of magnitude greater than for major pipelines: 1.5–2.0 per km.

FAILURE OF PIPE WITH SCAB AND SCRATCH

A scab is a surface defect of steel sheet in the form of an irregular dark spot produced by the rolling of a metal fragment welded to the slab on account of a casting error or adhesion during hot rolling (Fig. 1) [12, 17].

The scratch is a surface defect in the form of a channel without projecting edges and with a rounded

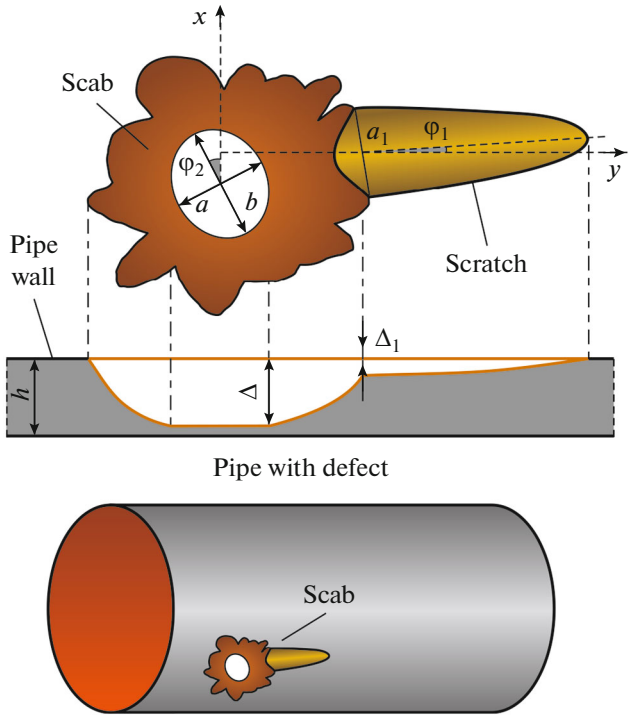

Fig. 2. Pipe with a scab and a scratch.

or flat base. It is formed as a result of scratching by the rolling system or by the motion of a solid over the sheet.

Suppose that p is the pressure in the pipe; h and D are the wall thickness and external diameter of the pipe ($h \ll D$); σ_u is the strength of the pipe; σ_y is its yield point; a and b are the longitudinal and transverse dimensions of the scab; Δ is the depth of the scab in the pipe wall ($\Delta < h$); a_1 and Δ_1 are the maximum width and depth of the scratch due to the scab ($\Delta_1 \le \Delta$); φ_1 is the inclination of the scab in the pipe cross section; and φ_2 is the inclination of the longitudinal axis of the scratch to the generatrix of the pipe (Fig. 2).

According to the theory of plastic flow, the deformation of elements of a continuum may be expressed as the sum of the ideally elastic strain and the incompressible rigid–plastic strain. The elastic strain corresponds to the generalized Hooke's law, and the plastic strain to St Venant–Mises theory.

Under the action of the internal pressure, we observe complex behavior of the pipe wall in the region of the scab and scratch: azimuthal extension, radial compression, and stress concentration.

According to St Venant–Mises theory, the outer wall of the pipe fails when the maximum tangential stress is half the strength σ_u.

In the case of a scab and scratch, the outer wall of the pipe fails at a critical pressure p_{sh}^{cr}

$$p \geq p_{sh}^{cr},$$
$$p_{sh}^{cr} = \sigma_u \Big/ \left| \mu \left\{ \frac{D}{2h} \left[1 + 2\left(\frac{\Delta - \Delta_1}{h - \Delta_1} \right) \right.\right.\right.$$
$$\left.\left.\left. \times \left(\sqrt{\frac{a}{b}} \cos\varphi_2 + \sqrt{\frac{b}{a}} \sin\varphi_2 \right) \right] \left(1 + 2\sqrt{\frac{2\Delta_1}{a_1}} \cos\varphi_1 \right) + 1 \right\} \right|,$$

where μ is a dimensionless empirical constant (μ = const ≥ 1).

Taking account of the scratch depth, we assess the stress concentration in the pipe wall due to the scab on the basis of the coefficient

$$K_1 = 1 + 2\left(\frac{\Delta - \Delta_1}{h - \Delta_1} \right) \left(\sqrt{\frac{a}{b}} \cos\varphi_2 + \sqrt{\frac{b}{a}} \sin\varphi_2 \right),$$

Likewise we assess the stress concentration in the pipe wall due to the width and depth of the scratch on the basis of the coefficient

$$K_2 = 1 + 2\sqrt{\frac{2\Delta_1}{a_1}} \cos\varphi_1.$$

The plastic deformation of the pipe wall begins at the pressure

$$p \geq p_{sh}^{pl},$$
$$p_{sh}^{pl} = \sigma_y \Big/ \left| \mu \left\{ \frac{D}{2h} \left[1 + 2\left(\frac{\Delta - \Delta_1}{h - \Delta_1} \right) \right.\right.\right.$$
$$\left.\left.\left. \times \left(\sqrt{\frac{a}{b}} \cos\varphi_2 + \sqrt{\frac{b}{a}} \sin\varphi_2 \right) \right] \left(1 + 2\sqrt{\frac{2\Delta_1}{a_1}} \cos\varphi_1 \right) + 1 \right\} \right|.$$

The Table 1 presents the critical pressures as a function of the depth Δ of the scab in the pipe wall ($h > \Delta \geq \Delta_1$) when

$$\mu = 1,\ D = 720\,\text{mm},\ h = 11\,\text{mm},\ \sigma_u = 684\,\text{MPa},$$
$$\sigma_y = 614\,\text{MPa},\ \Delta_1 = 3\,\text{mm},\ a = 20\,\text{mm},\ b = 25\,\text{mm},$$
$$a_1 = 20\,\text{mm},\ \varphi_1 = 10.4^\circ,\ \varphi_1 = 34.3^\circ,$$

FAILURE OF PIPE WITH SCAB BUT NO SCRATCH

In the case of a scab (but no scratch, $D_1 = 0$), the outer wall of the pipe fails at a critical pressure $p_{sh.pr}^{cr}$

$$p \geq p_{sh.pr}^{cr},$$
$$p_{sh.pr}^{cr} = \frac{\sigma_u}{\mu_1 \left\{ \frac{D}{2h} \left[1 + 2\frac{\Delta}{h} \left(\sqrt{\frac{a}{b}} \cos\varphi_2 + \sqrt{\frac{b}{a}} \sin\varphi_2 \right) \right] + 1 \right\}}.$$

Table 1. Dependence of the critical pressure on the depth of the scab in the pipe wall

Δ, mm	3	4	5	6	7	8	9	10
p_{sh}^{cr}, MPa	15.24	11.42	9.13	7.61	6.52	5.70	5.07	4.56
p_{sh}^{pl}, MPa	13.68	10.25	8.20	6.83	5.85	5.12	4.55	4.09

The plastic deformation of the pipe wall begins at the pressure

$$p \geq p_{sh.pr}^{pl} = \frac{\sigma_y}{\mu_1 \left\{ \frac{D}{2h} \left[1 + 2\frac{\Delta}{h} \left(\sqrt{\frac{a}{b}} \cos\varphi_2 + \sqrt{\frac{b}{a}} \sin\varphi_2 \right) \right] + 1 \right\}}.$$

EXAMPLE OF PIPE FAILURE

In Fig. 3, we show a steel pipe from a transfer pipeline with a defect that passes through the entire exterior wall. The working pressure when the accident occurred was p^{ru} = 4.4 MPa (59% of the design pressure of 7.5 MPa). The characteristics of the pipe are as follows: strength class K60; diameter 720 mm; wall thickness 11 mm; length 11.59 m; and mass 2.251 t. The pipe has a three-layer external insulating coating. The steel sheet for the pipe was produced by controlled rolling.

The scab and scratch correspond to local thinning of the pipe wall (dimensions 110 × 50 mm). With loss of sealing of the pipeline, the scab falls out, to form a hole passing through the entire wall (dimensions 20 × 25 mm), as shown in Fig. 4. The lost material has not been found. The smooth and undulatory surface of the defect shows that it is formed at a temperature comparable with the melting point of the sheet and is

Fig. 3. Scab on the outer surface of a pipe.

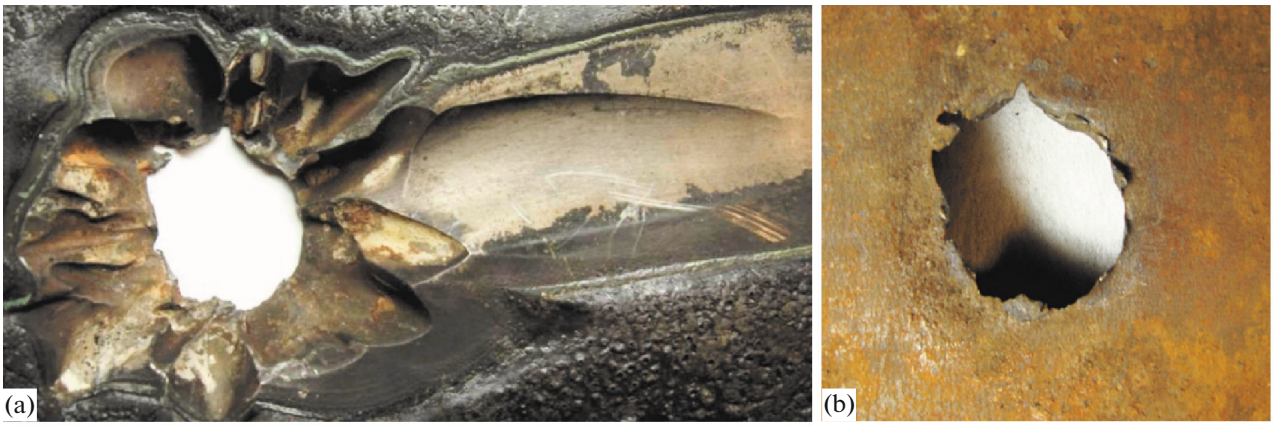

Fig. 4. Failed pipe: scab on external surface (a) and hole penetrating the wall to the inner surface (b).

deformed in hot rolling together with the sheet (Fig. 1).

The chemical composition and properties of the pipe wall correspond to strength class K60, according to Technical Specifications TU 1381-012-05757848–2005.

The pipe metal is metallographically analyzed at the central laboratory of the pipeline operator. To that end, three samples are cut from the pipe wall. The microstructure of the metal is determined by the etching of sections in 4% ethanolic nitric-acid solution. The microstructure of the pipe metal in all the sections consists of ferrite–pearlite grains of size 9–10, according to State Standard GOST 5630–82. The bands correspond to a score of 2B according to State Standard GOST 5640–68.

Fig. 5. Samples cut at the defect site, transverse (top) and parallel (bottom) to the rolling direction of the steel sheet.

The first sample is cut at the defect site in the plane transverse to the rolling direction (Fig. 5). The banding of the pearlite over the sample cross section is nonuniform. Local distortion of the pearlite banding is observed at the sample surface adjacent to the defect. Such structural distortion indicates that the defect was formed in hot deformation in the course of rolling. In view of the lack of pronounced bending over the length of the defective section and also its shape, we conclude that the defect is deformed in rolling together with the sheet.

The second sample is cut at the defect site in the plane parallel to the rolling direction (Fig. 5). Local distortion of the pearlite banding is observed.

The sample is cut at a distance of 300 mm from the defect site and is regarded as having the initial structure. The nonmetallic inclusions (point oxides) correspond to a size score of 2 according to State Standard GOST 1778–70 (scale A).

CAUSES OF SCABS

In our view, the dimensions and shape of the hole running through the wall of the ruptured pipe indicate that the scab and scratch may be formed when a hexagonal M12 nut (State Standard GOST 5915–70; width 19 mm; diagonal 21.94 mm; thickness 10 mm) or M14 nut (State Standard GOST 5927–70; width 21 mm; diagonal 24.25 mm; thickness 11 mm) falls onto the surface of the steel sheet in hot rolling (Fig. 1).

Before it is pressed into the hot sheet, the temperature of the nut will be considerably lower than that of the sheet. In rolling, the rollers do not immediately capture the nut, which consequently creates a scratch of increasing depth and width on the surface of the sheet. The maximum width of the scratch is equal to

the nut dimension at the instant that it is pressed into the sheet. The nut is pressed instantaneously into the surface of the hot sheet, with local increase in the metal temperature within the sheet wall so as to approximate the melting point of the metal. Some of the semiliquid metal is splashed onto the surface of the sheet. That accounts for the considerable increase in defect size in the direction of its external surface. Since the temperature of the elastic nut is still significantly lower than that of the sheet, the nut is easily pressed into the sheet over about half of its thickness. Once pressed into the sheet, the nut is rapidly heated to approximately the temperature of the sheet. When the nut and the sheet are rolled as a single mass in the subsequent rollers, the nut thickness is reduced, while its transverse dimensions are increased; it becomes oval.

ANALYSIS OF THE CRITICAL PRESSURE

The characteristics of the failed pipe are as follows

$$D = 720\,\text{mm},\ h = 11\,\text{mm},\ \sigma_u = 684\,\text{MPa},$$
$$\sigma_y = 614\,\text{MPa},\ \Delta_1 = 3\,\text{mm},\ a = 20\,\text{mm},\ b = 25\,\text{mm},$$
$$a_1 = 20\,\text{mm},\ \varphi_1 = 10.4^\circ,\ \varphi_1 = 34.3^\circ \text{ and } \Delta = 10\,\text{mm}.$$

At failure, the working pressure is $p^{ru} = 4.4$ MPa. Proceeding on the basis of our prior analysis, we find that, with the minimum value $\mu = 1$

$$p_{sh}^{cr} = 4.56\,\text{MPa},\ \frac{p_{sh}^{cr} - p^{ru}}{p^{ru}}.$$

Note that plastic deformation of the pipe wall begins somewhat earlier: when $p_{sh}^{pl} = 4.09$ MPa.

The calculation results for the failure of the pipe with a scab and scratch are consistent with the empirical data for a real pipe.

Note that, in the case of a pipe wall without defects (D = 720 mm; h = 11 mm; σ_u = 684 MPa, σ_y = 614 MPa), plastic deformation begins at an internal pressure $p_{pl} = 2h\sigma_y/D = 1876$ MPa, while failure occurs when $p_{cr} = 2h\sigma_u/D = 20.90$ MPa.

Given that the working gas pressure of the pipe at rupture was 4.4 MPa (4.4/20.9 = 21%), while the defect was so large as to be visible to the naked eye (110 × 50 mm), we conclude that ultrasonic monitoring and hydraulic testing of the pipe at the manufacturing plant must be improved.

CONCLUSIONS

We have developed means of calculating the critical internal pressure in a pipe with a scab and scratch on its outer surface as a function of the defect size and the strength of the steel pipe.

On that basis, we have analyzed a real incident in which a defect penetrated clean though the wall of a working pipeline.

The proposed approach may be used in the failure diagnostics of steel pipe in large- and medium-diameter gas and oil pipelines [12–36].

REFERENCES

1. *Micromanufacturing Engineering and Technology*, Qin, Y., Ed., Amsterdam: Elsevier, 2015, 2nd ed.
2. Klocke, F., *Manufacturing Processes 4. Forming*, New York: Springer-Verlag, 2013.
3. Lin, J., Balint, D., and Pietrzyk, M., *Microstructure Evolution in Metal Forming Processes*, London: Woodhead, 2012.
4. Banabic, D., *Sheet Metal Forming Processes. Constitutive Modeling and Numerical Simulation*, New York: Springer-Verlag, 2010.
5. Rees, D., *Basic Engineering Plasticity: An Introduction with Engineering and Manufacturing Applications*, Boston, MA: Butterworth-Heinemann, 2006.
6. Chakrabarty, J., *Theory of Plasticity*, Boston, MA: Butterworth-Heinemann, 2006.
7. Kang, S.-J., Sintering, in *Densification, Grain Growth, and Microstructure*, Boston, MA: Butterworth-Heinemann, 2004.
8. Bhattacharyya, D., *Composite Sheet Forming*, Amsterdam: Elsevier, 1997, vol. 11.
9. Predeleanu, M. and Gilormini, P., *Advanced Methods in Materials Processing Defects*, Amsterdam: Elsevier, 1997, vol. 45.
10. Abe, T. and Tsuruta, T., *Advances in Engineering Plasticity and Its Applications (AEPA'96)*, Amsterdam: Elsevier, 1996.
11. Predeleanu, M. and Ghosh, S.K., *Materials Processing Defects*, Amsterdam: Elsevier, 1995, vol. 43.
12. Bel'skii, S.M., Mazur, I.P., Lezhnev, S.N., and Panin, E.A., A two-zone model of browdening during rolling, *J. Chem. Technol. Metall.*, 2017, vol. 52, no. 2, pp. 180–185.
13. Muhin, U., Bel'skii, S., Makarov, E., and Koynov, T., Simulation of accelerated strip cooling on the hot rolling mill run-out roller table, *Frattura Integrita Strutturale*, 2016, vol. 37, pp. 305–311.
14. Muhin, U., Bel'skii, S., Makarov, E., and Koynov, T., Application of between- stand cooling in the production hot-rolled strips, *Frattura Integrita Strutturale*, 2016, vol. 37, pp. 312–317.
15. Muhin, U., Bel'skii, S., and Koynov, T., Study of the influence between the strength of antibending of working rolls on the widening during hot rolling of thin sheet metal, *Frattura Integrita Strutturale*, 2016, vol. 37, pp. 318–324.
16. Mazur, I.P. and Bel'skii, S.M., The St. Venant zone extent of the self-balancing longitudinal elastic stress, *Mater. Sci. Forum*, 2012, vol. 704-705, pp. 33–39.
17. Mukhin, Yu.A., Mazur, I.P., and Bel'skii, S.M., Determining the boundaries of the St. Venant zone for the self-balancing stress, *Steel Transl.*, 2007, vol. 37, no. 9, pp. 733–736.
18. Shinkin, V.N. and Kolikov, A.P., Simulation of the shaping of blanks for large-diameter pipe, *Steel Transl.*, 2011, vol. 41, no. 1, pp. 61–66.

19. Shinkin, V.N. and Kolikov, A.P., Elastoplastic shaping of metal in an edge-bending press in the manufacture of large-diameter pipe, *Steel Transl.*, 2011, vol. 41, no. 6, pp. 528–531.
20. Shinkin, V.N. and Kolikov, A.P., Engineering calculations for processes involved in the production of large-diameter pipes by the SMS Meer technology, *Metallurgist*, 2012, vol. 55, nos. 11–12, pp. 833–840.
21. Shinkin, V.N., The mathematical model of the thick steel sheet flattening on the twelve-roller sheetstraightening machine. Massage 1. Curvature of sheet, *CIS Iron Steel Rev.*, 2016, vol. 12, pp. 37–40.
22. Shinkin, V.N., The mathematical model of the thick steel sheet flattening on the twelve-roller sheet-straightening machine. Massage 2. Forces and moments, *CIS Iron Steel Rev.*, 2016, vol. 12, pp. 40–44.
23. Shinkin, V.N., Geometry of steel sheet in a seven-roller straightening machine, *Steel Transl.*, 2016, vol. 46, no. 11, pp. 776–780.
24. Shinkin, V.N., Preliminary straightening of thick steel sheet in a seven-roller machine, *Steel Transl.*, 2016, vol. 46, no. 12, pp. 836–840.
25. Maksimov, E.A. and Shatalov, R.L., Asymmetric deformation of metal and front flexure of thick sheet in rolling. Part 2, *Steel Transl.*, 2012, vol. 42, no. 6, pp. 521–525.
26. Matrosov, Yu.I., Levchenko, V.I., Loskutov, A.Yu., Volodarskii, V.V., Kolyasnikova, N.V., and Talanov, O.P., Influence of pipe processing on the mechanical properties of K60 steel sheet, *Steel Transl.*, 2012, vol. 42, no. 6, pp. 536–540.
27. Maksimov, E.A. and Shatalov, R.L., Asymmetric deformation of metal and front flexure of thick sheet in rolling. Part 1, *Steel Transl.*, 2012, vol. 42, no. 5, pp. 442–446.
28. Groshkova, A.L., Polulyakh, L.A., Travyanov, A.Ya., Dashevskii, V.Ya., and Yusfin, Yu.S., Phosphorus distribution between phases in smelting high-carbon ferromanganese in the blast furnace, *Steel Transl.*, 2007, vol. 37, no. 11, pp. 904–907.
29. Podgorodetskii, G.S., Yusfin, Yu.S., Sazhin, A.Yu., Gorbunov, V.B., and Polulyakh, L.A., Production of generator gas from solid fuels, *Steel Transl.*, 2015, vol. 45, no. 6, pp. 395–402.
30. Orelkina, O.A., Petelin, A.L., and Polulyakh, L.A., Distribution of secondary gas emissions around steel plants, *Steel Transl.*, 2015, vol. 45, no. 11, pp. 811–814.
31. Polulyakh, L.A., Dashevskii, V.Ya., and Yusfin, Yu.S., Manganese-ferroalloy production from Russian manganese ore, *Steel Transl.*, 2014, vol. 44, no. 9, pp. 617–624.
32. Kovalev, A.I., Vainshtein, D.L., Rashkovskii, A.Yu., Khlusova, E.I., and Orlov, V.V., Features of structural changes through the cross section of sheet rolled from high strength skelp steels, *Metallurgist*, 2011, vol. 55, nos. 1–2, pp. 34–45.
33. Morozov, Yu.D., Naumenko, A.A., and Lyasotskii, I.V., Effect of rolling heating and deformation and accelerated cooling regimes on mechanical property formation for rolled steel sheet of strength class Kh80, *Metallurgist*, 2011, vol. 54, nos. 9–10, pp. 686–695.
34. Manzhurin, I.P. and Sidorina, E.A., Dependence of the surface deformation of strip on the parameters of its shaping, *Metallurgist*, 2012, vol. 56, nos. 1–2, pp. 37–42.
35. Nikitin, G.S., Galkin, M.P., and Zhikharev, P.Yu., Effect of noncontact zones on the deforming forces in metal-shaping operations, *Metallurgist*, 2013, vol. 56, nos. 9–10, pp. 766–772.
36. Salganik, V.M., Chikishev, D.N., Pustovoitov, D.O., Denisov, S.V., and Stekanov, P.A., Developing regimes for the asymmetric rolling of low-alloy steel plates to minimize bending of the ends of the plate, *Metallurgist*, 2014, vol. 57, nos. 11–12, pp. 1005–1008.

Translated by Bernard Gilbert